LIMNOLOGY and OCEANOGRAPHY

ASLO

Limnol. Oceanogr. 9999, 2025, 1–15

doi: 10.1002/lno.70273

RESEARCH ARTICLE

Carbon fluxes in two temperate ponds are mediated by stratification and primary producers

Meredith A. Holgerson,[1*] **Nicholas E. Ray**,[1,2] **Kathryn A. Gannon**,[1,3] **Adam J. Heathcote**[4]

[1]Department of Ecology and Evolutionary Biology, Cornell University, Ithaca, New York, USA; [2]School of Marine Science and Policy, University of Delaware, Lewes, Delaware, USA; [3]Department of Ecology and Evolutionary Biology, Institute of Arctic and Alpine Research, University of Colorado, Boulder, Colorado, USA; [4]St. Croix Watershed Research Station, Science Museum of Minnesota, Marine on St. Croix, Minnesota, USA

Abstract

Ponds influence global carbon (C) cycling due to high rates of organic C (OC) burial and carbon dioxide (CO_2) and methane (CH_4) emissions. Here, we quantified OC burial rates and CO_2 and CH_4 concentrations and fluxes in two ponds that were similar in size and gross primary production, but differed in depth and dominant primary producers. The deeper (3.9 m) Texas Hollow Pond was phytoplankton dominated with stronger and longer (143 d) stratification compared to the shallower (2.7 m) macrophyte-dominated Mud Pond (85 d). Both ponds exhibited high CO_2 and CH_4 emissions and high OC burial, yet C pathways differed. Strong stratification in Texas Hollow Pond led to anoxic bottom waters, benthic CO_2 and CH_4 accumulation, and limited OC decomposition, whereas Mud Pond remained oxygenated with similar gas concentrations across the water column. Texas Hollow Pond had 2.6 times higher CO_2 emissions than Mud Pond, perhaps related to greater wetland C inputs in Texas Hollow. Despite similar diffusive CH_4 emissions between ponds, the weakly stratified Mud Pond had twice as much CH_4 ebullition, likely due to warmer waters and macrophyte-derived OC fueling methanogenesis. In summary, slight differences in depth and light attenuation can regulate stratification, plant communities, oxygen availability, and C processing in ponds. Given that ponds are hotspots for C cycling and are sensitive to climate-driven changes in stratification, understanding the mechanisms behind C processing is critical for local management and predicting global C budgets.

Small inland freshwaters are an important component of global carbon (C) and greenhouse gas (GHG) budgets (Holgerson and Raymond 2016; Rosentreter et al. 2021). Lakes and ponds sequester organic C (OC) in sediments and exchange carbon dioxide (CO_2) and methane (CH_4) with the atmosphere. Small lakes and ponds have an outsized role in C cycling due to greater allochthonous inputs relative to their water volume (Downing 2010) and high metabolic rates (Rabaey et al. 2024). As a result, ponds (< 0.05 km^2 and < 5 m deep; Richardson et al. 2022) emit more GHGs and store more OC than larger lakes on an areal basis (Downing et al. 2008; Downing 2010; Rosentreter et al. 2021). While it is clear that small lakes and ponds are important in global C budgets, substantial uncertainty remains in predicting rates of OC burial and GHG emissions both for individual waterbodies and at the global scale (Deemer and Holgerson 2021; Ray et al. 2023; Holgerson et al. 2024). Better characterization of the physical, chemical, and biological properties that predict GHG cycling in ponds will reduce uncertainty and inform global upscaling efforts.

Depth and light availability are two physical variables that regulate C cycling in ponds by influencing stratification (Fee et al. 1996; Holgerson et al. 2022; Søndergaard et al. 2023) and primary producers (Søndergaard et al. 2013). While shallow waterbodies were once thought to be well mixed, recent work emphasizes that with sufficient depth, ponds can stratify for days, weeks, or months at a time (Holgerson et al. 2022; Søndergaard et al. 2023). Stratification can regulate rates of organic matter decomposition, GHG production, and CH_4 consumption by influencing bottom water temperatures and anoxia (Bartosiewicz et al. 2019; Ray et al. 2023; Rabaey and Cotner 2024). First, stratification can thermally shield

*Correspondence: meredith.holgerson@cornell.edu

Associate editor: Werner Eckert

bottom waters, slowing methanogenesis and organic matter decomposition (Bartosiewicz et al. 2019). Stratification also promotes anoxic bottom waters under high nutrient or C concentrations (LaBrie and Maranger 2024), further slowing total organic matter decomposition while increasing methanogenesis (Sobek et al. 2009; Bartosiewicz et al. 2019). In shallow waters, effects from anoxia may outweigh those from thermal shielding as stratification has promoted diffusive and ebullitive CH_4 fluxes in ponds and shallow lakes (Ray and Holgerson 2023; Davidson et al. 2024; Rabaey and Cotner 2024). Stratification may also impact $CO_2 : CH_4$ emissions ratios, favoring high $CO_2 : CH_4$ under oxic, mixed conditions (Bartosiewicz et al. 2015).

Depth and light also influence the dominant type of primary producers in ponds, with implications for C cycling. Shallower and clearer waters are more likely to be macrophyte dominated, whereas deeper or darker waters can limit light reaching sediments, resulting in phytoplankton dominance (Scheffer et al. 1993). These differing plant communities could alter the quantity and quality of organic matter loaded into sediments, thereby influencing burial and GHG production (Hilt et al. 2017; Baliña et al. 2023; Bauduin et al. 2025). It is uncertain how C cycling differs in phytoplankton- or macrophyte-dominated states because few studies have contrasted the balance of both OC burial and GHG emissions across these systems (Hilt et al. 2017).

To better characterize C cycling in ponds, we measured annual rates of GHG emissions and OC burial in two natural ponds that were similar in size, but differed in stratification and dominant primary producers. We hypothesized that the deeper, phytoplankton-dominated pond with stronger stratification would develop anoxic bottom waters leading to the buildup of GHGs and reduced decomposition, thereby increasing OC burial rates. In contrast, we hypothesized that the shallower pond with weaker and shorter stratification would have an oxic water column, leading to lower CH_4 production and emissions, greater CO_2 emissions, and lower OC burial rates.

Methods

Study sites

We studied two glacier-formed ponds, Mud Pond and Texas Hollow Pond, located within temperate deciduous forests of central New York State. Both ponds are in hollows, similar in elevation (336–362 m), surface area (0.4–0.5 ha of open water), and are each immediately surrounded by emergent wetland (Table 1). Mud Pond is shallower, with a maximum depth (z_{max}) of 2.7 m, and submerged macrophytes (*Ceratophyllum demersum*, *Elodea canadensis*, and *Chara vulgaris*) grow throughout its basin. Mud Pond is fed from a permanent or intermittent stream, and its 131-ha catchment is 45% agricultural, 27% forest, and 20% wetland land cover. In contrast, Texas Hollow Pond is deeper (z_{max}: 3.9 m) and macrophytes (primarily *Potamogeton pusillus*) are limited to shallow edges, with greater algal biomass (estimated via chlorophyll *a*) in surface waters. Texas Hollow Pond has a smaller (48 ha) catchment that contains 68% forest, 15% agricultural, and 13% wetland land cover, and the pond lacks permanent inflows or outflows. Both ponds had minimal (< 0.25 m) changes in z_{max} over the study. We surveyed each pond's bathymetry using a portable depth sounder (Hondex, Honda Electronics; Fig. 1). We collected one sediment core from each pond in August 2021, with all other sampling occurring during the 2022 open-water season from late April through mid-November when ice began to form.

Table 1. Characteristics of the two study ponds. Water chemistry values represent seasonal averages of surface waters with ranges in parentheses. The surface area is of open water, with the surrounding wetland complex area representing the surface area of adjacent emergent wetlands estimated from aerial imagery.

	Texas Hollow Pond	Mud Pond
Latitude	42.41363	42.54674
Longitude	−76.7874	−76.2664
Elevation (m)	362	336
Surface area (ha)	0.53	0.40
Surrounding wetland complex (ha)	3.393	2.470
Catchment area (ha)	47.84	131.35
Maximum depth (m)	3.9	2.7
Surface pH	7.52 (6.45–8.47)	7.92 (7.43–8.53)
Surface chlorophyll *a* (μg L^{-1})	12.5 (0.35–21.60)	1.26 (0.14–2.80)
Soluble reactive phosphorus (mg L^{-1})	0.004 (0.001–0.007)	0.002 (0.001–0.004)
Nitrate (mg L^{-1})	0.003 (0.001–0.003)	0.683 (0.447–1.510)
Ammonium (mg L^{-1})	0.006 (0.002–0.022)	0.105 (0.026–0.212)
Total dissolved nitrogen (mg L^{-1})	0.403 (0.23–0.53)	0.811 (0.56–1.44)
DOC (mg L^{-1})	14.5 (11.8–15.7)	22.4 (12.7–34.2)

Water column stratification

We deployed buoys with thermistor chains in late April 2022, with thermistors (HOBO pendants and ProV2s) placed at 0.2, 0.7, 1.7, and 2.4 m from the surface in Mud Pond and at 0.2, 1.5, 2.5, and 3.7 m from the surface in Texas Hollow Pond. Thermistors recorded water temperature every 10 min. In Mud Pond, the surface thermistor was accidentally set to log hourly beginning 11 July; we interpolated to 10 min temperature measurements for analyses. In Texas Hollow Pond, the buoy was accidentally moved to a shallower location from 14 June to 16 August so we used sonde data (approximately weekly) from this time to interpolate temperature below 1.5 m. We classified each time point as "mixed" or "stratified"

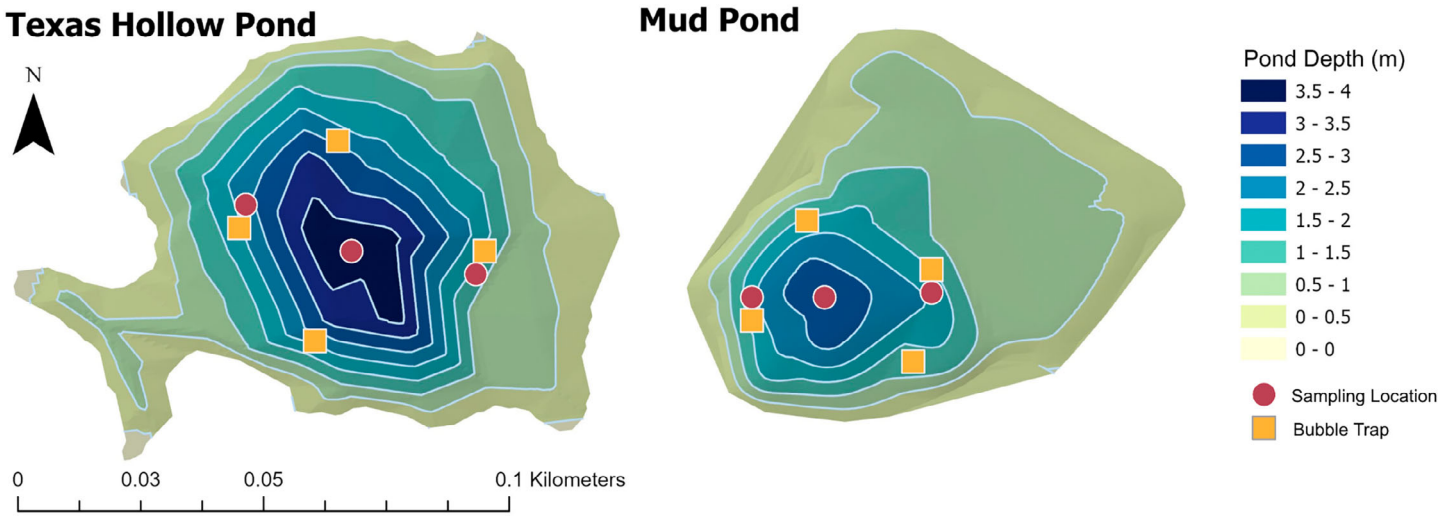

Fig. 1. Bathymetric maps of Mud Pond and Texas Hollow Pond. Color gradations and contour lines denote 0.5 m depth differences. Maroon circles mark sampling locations and orange squares mark the four bubble traps.

using a threshold density difference between the top and bottom sensor of 0.35 kg m^{-3} based on visual inspections of temperature plots (Fig. 2; Supporting Information Fig. S1). While there is no agreed upon threshold value to classify mixing, our number was slightly larger than values used to calculate mixing depth in lakes as reviewed by Gray et al. (2020) and slightly lower than the density gradients used for ponds by Holgerson et al. (2022). We calculated the Relative Thermal Resistance to Mixing (RTRM) to compare stratification strength through time (Wetzel and Likens 2000).

Environmental parameters

We sampled surface waters for dissolved nutrients (NO_3^-, NH_4^+, soluble reactive phosphorus [SRP]), dissolved organic carbon (DOC), total dissolved nitrogen (TDN), and chlorophyll *a* in late April and every 3–4 weeks from early June through mid-November ($n = 9$ per pond). We filtered (0.7 μm GF/F) water into acid-washed polyethylene bottles, which were frozen prior to analysis of dissolved nutrients. We collected chlorophyll *a* samples on GF/F filters, which were frozen until analysis using standard fluorometric protocols (Yentsch and Menzel 1963). Dissolved nutrients were analyzed at the Academy of Natural Sciences at Drexel University using a KPM SmartChem 200 Discrete Analyzer for NO_3^- and SRP and a SEAL Analytical AA500 Continuous Flow Analyzer for NH_4^+. Minimum detection limits were 0.008 mg L^{-1} for NH_3/NH_4^+, 0.002 mg L^{-1} for NO_3^-/NO_2^- and 0.004 mg L^{-1} for SRP. We analyzed DOC and TDN using a total carbon analyzer (Shimadzu TOC-LCSN).

We used a sonde (Eureka Manta + 35; Eureka Water Probes) to measure water column profiles (every 0.25 m) for dissolved oxygen (DO) concentrations, temperature, pH, conductivity, chlorophyll *a*, NO_3^-, NH_4^+, and photosynthetically active radiation (PAR) about weekly through the study ($n = 21$ d per pond). For each pond and sampling day, we calculated the light attenuation coefficient (K_d) as the slope of a linear regression model of PAR (natural log) vs. depth. As we noticed obvious water color differences between ponds, we measured true and apparent color in 2024 (Hach water color test kit).

We deployed one DO logger (miniDOT; PME) in the upper mixed layer of each pond, placed at 0.5 m in Mud Pond and 0.7 m in Texas Hollow Pond. The loggers recorded DO and temperature every 10 min from 28 April (Mud) or 5 May (Texas Hollow) through 15 October 2022.

Calculating bathymetry and anoxia metrics

We calculated bathymetry from location, depth, and pond polygon data using ArcGIS (ArcGIS Pro 2.9.0). We used the interp package (Gebhardt 2024) in R (R Core Team 2020) to fit a triangular irregular network surface model to interpolate depth for each 1 × 1 m grid cell across each pond polygon. We used these models to calculate the surface area of the pond for each 0.25 m depth layer.

For each gas sampling date, we calculated the volume of water that was hypoxic (DO < 2 mg L^{-1}) and the proportion of the pond's surface area with anoxic sediments, termed the anoxic fraction. The anoxic fraction includes all sediments underlying hypoxic waters (Nürnberg 1987).

Modeling ecosystem metabolism

To assess if ponds differed in productivity, we estimated volumetric gross primary production (GPP), ecosystem respiration (ER), and net ecosystem production (NEP) using the maximum likelihood method in the LakeMetabolizer R package (Winslow et al. 2016). Model inputs included pond DO and temperature data and PAR from a central weather station (≤ 30 km from the ponds). Models predicted mixing depth from the temperature data and were run daily from sunrise to

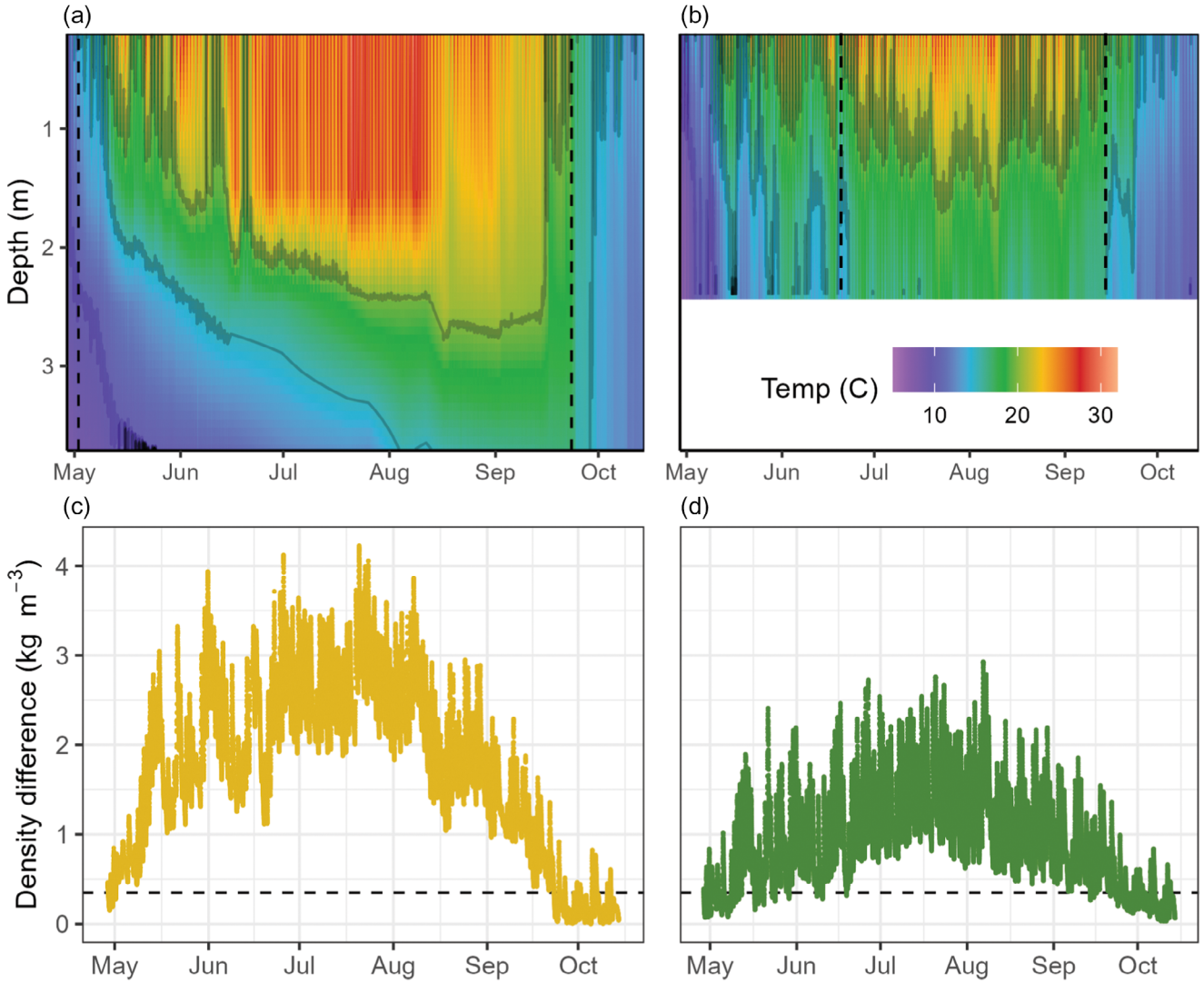

Fig. 2. Water column stratification for Texas Hollow Pond (left; gold) and Mud Pond (right; green). (**a**) and (**b**) show interpolated heat maps of water temperature from four thermistors located across the water column (*see* Fig. S1 for temperature line plots), with gray contour lines at 10, 15 and 20°C. (**c**) and (**d**) show density differences for the ponds, with the dashed line at 0.350 kg m^{-3} delineating the mixing threshold.

sunrise. We assumed a constant k_{600} value of 0.51 m d^{-1} based on the average value for 30 waterbodies < 0.1 km^2 in Holgerson et al. (2017), and similar to the 0.50 m d^{-1} proposed for wind-sheltered lakes < 0.5 km^2 (Cole et al. 2010). As both ponds are located in hollows and surrounded by forest, wind speed was typically < 3 m s^{-1}, where wind speed models often break down (Cole and Caraco 1998; Vachon and Prairie 2013). In a study modeling metabolism for 35 shallow freshwater ponds and lakes, a constant k_{600} yielded similar model fits to using a wind-based k_{600}, further supporting our approach (Rabaey et al. 2024). We filtered data based on "good" or "bad" fits similar to Rabaey et al. (2024) and excluded impossible values (e.g., ER > 0 or GPP < 0), resulting in good model fits for 26 d in Mud Pond and 47 d in Texas Hollow Pond. Poor model fits primarily related to mixing in Mud Pond and diel anoxia in Texas Hollow, which are common challenges when modeling metabolism in shallow systems (Rabaey et al. 2024).

Carbon burial measurements

We collected one sediment core each from the z_{max} of Mud Pond (92 cm) and Texas Hollow Pond (122 cm) in August 2021 using a rod-driven piston corer (Fig. 1; Wright 1991). We sectioned each core vertically on site at 1 cm increments and froze subsamples until subsequent analysis.

We measured ^{210}Pb activity at 17–20 depth intervals from each core to determine age and sediment accumulation rates via alpha spectrometry following the methodology of Eakins and Morrison (1978) on an alpha spectroscopy system (Ortec). We estimated dates and dry mass accumulation rates (DMAR) using the constant rate of supply model with errors

calculated by first-order propagation of counting uncertainty (Appleby 2001). We focus-corrected DMAR to whole-pond estimates by calculating a focus factor from the annual flux of ^{210}Pb measured at the core site divided by measured atmospheric ^{210}Pb deposition rates from the northeastern USA (0.77 pCi cm^{-2} yr^{-1}; Muir et al. 2009).

The percent organic matter content of each section was estimated by loss-on-ignition and converted to percent OC via a correction factor of 0.469 (Dean 1974). We calculated OC burial via the product of the percent OC and focus-corrected DMAR for each section (Heathcote and Downing 2012) and excluded sediment intervals < 10 yr in age to minimize the effect of incomplete diagenesis (Heathcote et al. 2015).

Greenhouse gas sampling

We sampled for dissolved GHG concentrations on 28 April and then every 3–4 weeks from early June through mid-November, with one extra sampling during fall mixing ($n = 10$ sampling days per pond). We collected triplicate air samples and collected surface water samples at three locations to capture spatial variability (Fig. 1). We also collected one bottom water sample ~ 0.25 m above the sediments at z_{max} using a Van Dorn sampler. We used a headspace equilibration approach with ambient air and stored the headspace gas in pre-evacuated exetainers for later analysis on a gas chromatograph equipped with an electron capture detector (ECD) and flame ionization detector (FID) with methanizer (Shimadzu GC 2014). We used ambient air concentrations from each site and date to determine partial pressures for each gas in the initial headspace composition before equilibration after removing 16 samples (of 180) where an ambient air concentration appeared to be an outlier (over double the median standard deviation and unlike other replicates). We determined atmospheric pressure based on elevation and temperature. We then calculated dissolved CO_2 and CH_4 concentrations for each sample following Henry's law and the ideal gas law using constants determined by Weiss (1974) and Wiesenburg and Guinasso (1979).

We measured ebullitive CH_4 emissions from 13 June through 15 November using four passive bubble trap samplers deployed to capture spatial variability (Fig. 1). Bubble traps consisted of a funnel attached to an inverted graduated cylinder held in a float, where accumulated bubbles displaced water, allowing us to measure volume over time (Ray and Holgerson 2023). We checked and reset traps every few days to every few weeks depending on ebullition rates ($n = 28$ dates for Mud Pond and $n = 18$ for Texas Hollow). We collected gas from at least one bubble trap per pond for later analysis of CH_4 concentration, although we acknowledge that bubble CH_4 concentrations can vary across waterbodies (Wik et al. 2013; Kuhn et al. 2023). When enough gas permitted, we collected 20 mL of gas, which we stored and analyzed similar to dissolved gas concentrations using a dilution factor of 30. We analyzed the average volume of accumulated gas across all traps in a pond on a given day. On sampling dates where we did not collect any bubble samples ($n = 8$) or samples were compromised ($n = 2$), we used the seasonal average CH_4 concentration by pond (49.9% for Mud; 64.5% for Texas Hollow). We calculated ebullitive emissions as:

$$\text{Ebullitive flux}\left(\text{mmol m}^{-2}\text{d}^{-1}\right) = \frac{[CH_4] \times V \times P}{A \times \Delta t \times R \times T_{\text{water}}}$$

where $[CH_4]$ is the concentration of CH_4 in the bubble (μL L^{-1}), V is the bubble volume (L), P is pressure derived from elevation and temperature (atm), A is basal area of the bubble trap (m^2), Δt is deployment time (d), R is the universal gas constant (0.08206 L atm K^{-1} mol^{-1}), T_{water} is the water temperature (K) at the sampling time.

Greenhouse gas flux estimates

We estimated diffusive GHG emissions using dissolved gas concentrations and estimates of gas transfer velocity:

$$\text{Flux}\left(\text{mmol m}^{-2}\text{h}^{-1}\right) = k\left(\text{m h}^{-1}\right) \times \left(\text{Conc}_{\text{surf}} - \text{Conc}_{\text{eq}}\right)$$

where k is the gas transfer velocity for a given gas, $\text{Conc}_{\text{surf}}$ is the gas concentration in the surface water (mmol m^{-3}), Conc_{eq} is the gas concentration in the water if it were in equilibrium with the air (mmol m^{-3}). We used atmospheric partial pressure and Henry's law to calculate Conc_{eq} for each gas on each sampling date.

The gas transfer velocity was calculated according to Wanninkhof (1992):

$$k_{\text{gas2}} = \frac{k_{600}}{\left(\frac{600}{Sc_{\text{gas2}}}\right)^{n}}$$

where k_{600} is the k for CO_2 at 20°C and Sc is the Schmidt number of a gas for a particular water temperature and density. As described above for ecosystem metabolism, we assumed a k_{600} value of 0.51 m d^{-1}. We calculated Sc for CH_4 and CO_2 following equations from Wanninkhof (1992). We used an exponent n value of −0.67, which is appropriate for low-wind environments (Jähne et al. 1987; Matthews et al. 2003).

Calculating annual carbon fluxes

We estimated annual C emissions for each pond by numerically integrating diffusive and ebullitive GHG fluxes over time using the AUC command in the DescTools package in R (Signorell 2024) with a trapezoidal method for diffusive fluxes and step method for ebullitive fluxes (Ray and Holgerson 2023). As our ebullitive flux measurements started 13 June, we linearly extrapolated earlier fluxes based on a conservative assumption of no ebullition at the start of gas concentration sampling on 28 April. We assumed flux was constant over a 24-h period, and assumed fluxes were 0 over

the winter, which is conservative as ice cover was not continuous and ice melt occurred before the first sampling on 28 April. We estimated emissions from fall mixing in Texas Hollow Pond using the total CH_4 accumulated in the hypoxic hypolimnion just prior to mixing, and assumed all of it vented to the atmosphere (i.e., no CH_4 oxidation). We did not include fall turnover estimates from Mud Pond as CH_4 did not accumulate in bottom waters.

Results

Water column stratification

Texas Hollow Pond stratified from 2 May to 22 September, resulting in 143 d of continual stratification (Fig. 2). In contrast, Mud Pond stratified for 85 d from 20 June to 13 September (Fig. 2). Texas Hollow Pond had higher surface temperatures (average difference +2.7°C from May to August) and cooler bottom waters (average difference −3.2°C between May and August) than Mud Pond. As a result, stratification strength (measured by RTRM) averaged 1.83 times greater in Texas Hollow than Mud Pond in July and August when both ponds were stratified (Supporting Information Fig. S2).

Water chemical and biological parameters

Texas Hollow Pond had consistently higher surface chlorophyll *a* concentrations compared to Mud Pond (Table 1; Supporting Information Fig. S3). While surface DOC concentrations were higher in Mud Pond, we observed clear water in Mud Pond and visibly stained waters in Texas Hollow Pond. When we measured water color in 2024, both true and apparent color were three times higher in Texas Hollow Pond. Higher chlorophyll *a* concentrations and stained water explain the greater light attenuation in Texas Hollow Pond, with K_d values (1.75 ± 0.10 [SE] m^{-1}) more than double that of Mud Pond (0.78 ± 0.15 m^{-1}). Despite macrophyte coverage that likely influenced PAR readings, Mud Pond was entirely euphotic whereas the compensation depth of Texas Hollow averaged 2.63 m with no PAR reaching bottom waters. Differences in K_d help explain why sonde chlorophyll *a* readings were typically highest toward the bottom of Mud Pond, whereas Texas Hollow developed a deep chlorophyll maximum between 2 and 3 m in late June, which persisted through to water column mixing in September.

Mud Pond had consistently higher surface water concentrations of NH_4^+, NO_3^-, and TDN (Table 1; Supporting Information Fig. S3). Our water column profiles show that Mud Pond had similar NH_4^+ and NO_3^- concentrations throughout the water column or sometimes values were higher in surface waters, whereas NH_4^+ accumulated at the bottom of Texas Hollow Pond during summer stratification.

pH was similar in surface waters of Mud Pond (7.92 ± 0.05 SE) and Texas Hollow Pond (7.53 ± 0.11; Table 1), but pH decreased with depth in Texas Hollow. The bottom waters of Texas Hollow (3.5 m) had an average pH of 6.3 ± 0.11 (SE) compared to 7.8 ± 0.06 in Mud.

The oxygen availability differed greatly between the two ponds. Texas Hollow had a hypoxic hypolimnion, with the depth to hypoxia (2 mg L^{-1}) typically between 2 and 2.75 m (Fig. 3). The anoxic fraction, or proportion of the pond's surface area with anoxic surface sediments, reached 0.44 in July prior to a partial mixing event, and then reached 0.31 prior to fall mixing in September (Supporting Information Fig. S4). Before fall mixing, we estimate that 21% of the water volume was hypoxic. In contrast, Mud Pond was often supersaturated in oxygen and we never observed anoxia in the water column.

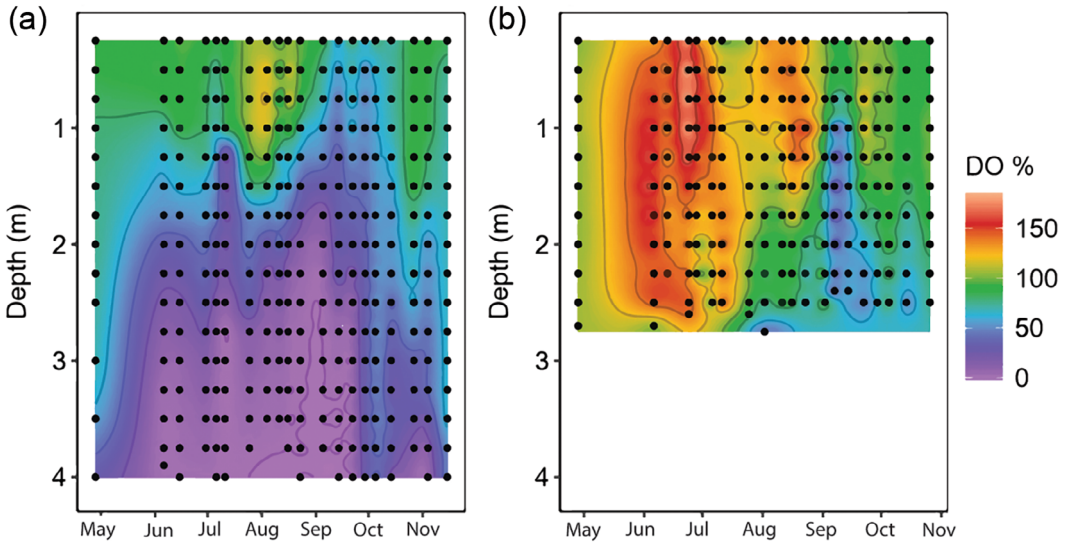

Fig. 3. Seasonal sonde snapshots (black dots) interpolated to show dissolved oxygen (% saturation) throughout the water column of (**a**) Texas Hollow Pond and (**b**) Mud Pond. Cooler colors denote oxygen undersaturation, whereas warmer colors denote supersaturation.

Ecosystem metabolism

Mud Pond had slightly higher GPP (3.89 ± 0.53 [SE] g O_2 m^{-3} d^{-1}) than Texas Hollow (2.91 ± 0.24 g O_2 m^{-3} d^{-1}; Fig. 4b). Both ponds tended to be more productive late summer, with the peak in Mud Pond exceeding Texas Hollow in late August and early September. Texas Hollow Pond had consistently greater ER rates (-4.55 ± 0.36 g O_2 m^{-3} d^{-1}) compared to Mud Pond (-3.78 ± 0.52 g O_2 m^{-3} d^{-1}) (Fig. 4c,d), leading to heterotrophic conditions in Texas Hollow and slight autotrophic conditions in Mud (Fig. 4e,f).

Carbon burial

Our model estimates of OC burial rates in the two ponds were similar, despite markedly different organic matter content and DMAR. Sediments in Texas Hollow Pond had more than double the organic matter (70.5 ± 1.41 [SE] %) than those in Mud Pond (26.4 ± 0.22%; Fig. 5a). There were two dips in organic matter content in Texas Hollow Pond reflecting visible lithologic anomalies associated with terrigenic (clay and sand) inputs, which correspond to and plausibly relate to the timing of 100-yr floods in the region in 1935 and 1956. Through time, the sediment DMAR was relatively steady in Texas Hollow Pond, whereas DMAR increased in Mud Pond, resulting in Mud Pond having more than double the accumulation rates than Texas Hollow Pond in recent decades (Fig. 5b). Rates of OC burial tended to be higher in Texas Hollow Pond through time; however, differences in organic matter content and DMAR counteracted each other to reduce differences in recent years. From 1975 to 2000, the OC burial rate averaged 182.9 ± 3.0 (SE) g OC m^{-2} yr^{-1} in Mud Pond and 245.5 ± 11.5 g OC m^{-2} yr^{-1} in Texas Hollow Pond (Fig. 5c; Supporting Information Fig. S5).

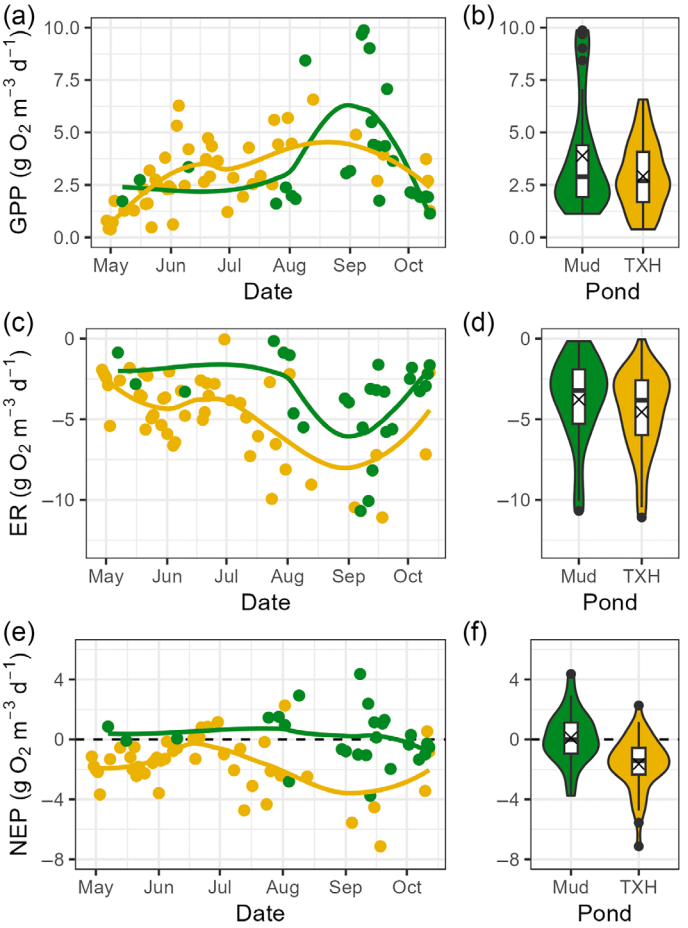

Fig. 4. Daily estimates of (**a**) gross primary production (GPP), (**c**) ecosystem respiration (ER), and (**e**) net ecosystem production (NEP) in Mud Pond (green) and Texas Hollow Pond (TXH; gold). Lines visualize locally estimated scatterplot smoothing (loess). Violin boxplots depict seasonal data of (**b**) GPP, (**d**) ER, and (**f**) NEP. Violin plots illustrate the distribution of the data; boxplots show the median (middle bar), 25th and 75th percentiles (bottom and top horizontal lines), values beyond 1.5× the interquartile range (points), and averages (X symbol). Black dashed lines in (e) and (f) represent the transition between net autotrophy and heterotrophy (NEP = 0).

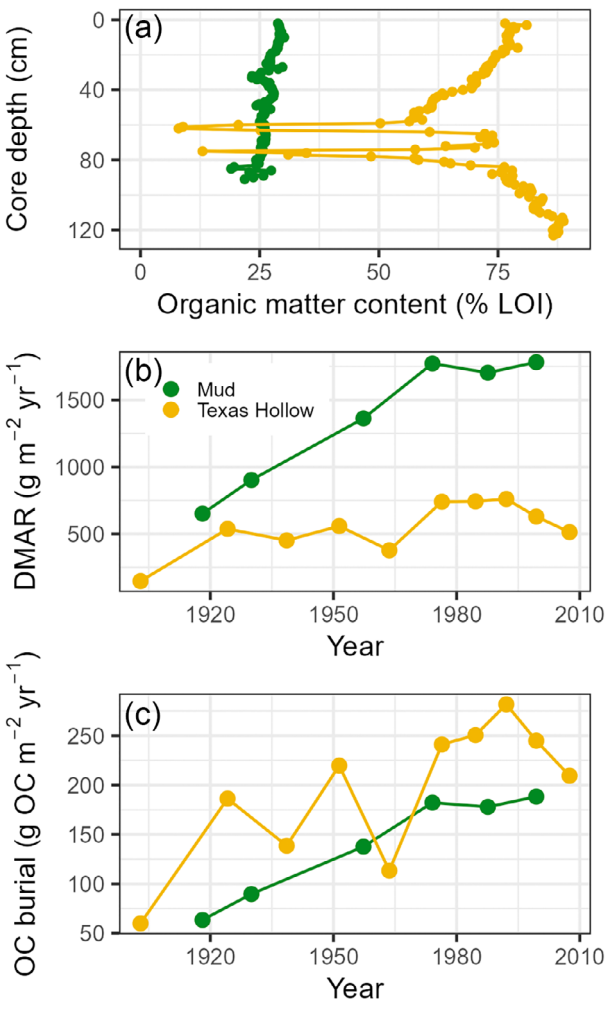

Fig. 5. Sediment carbon characteristics for Texas Hollow Pond (gold) and Mud Pond (green). (**a**) Organic matter content based on loss-on-ignition (LOI) through the sediment core, (**b**) dry mass accumulation rates (DMAR) through time, and (**c**) organic carbon (OC) burial rates through time.

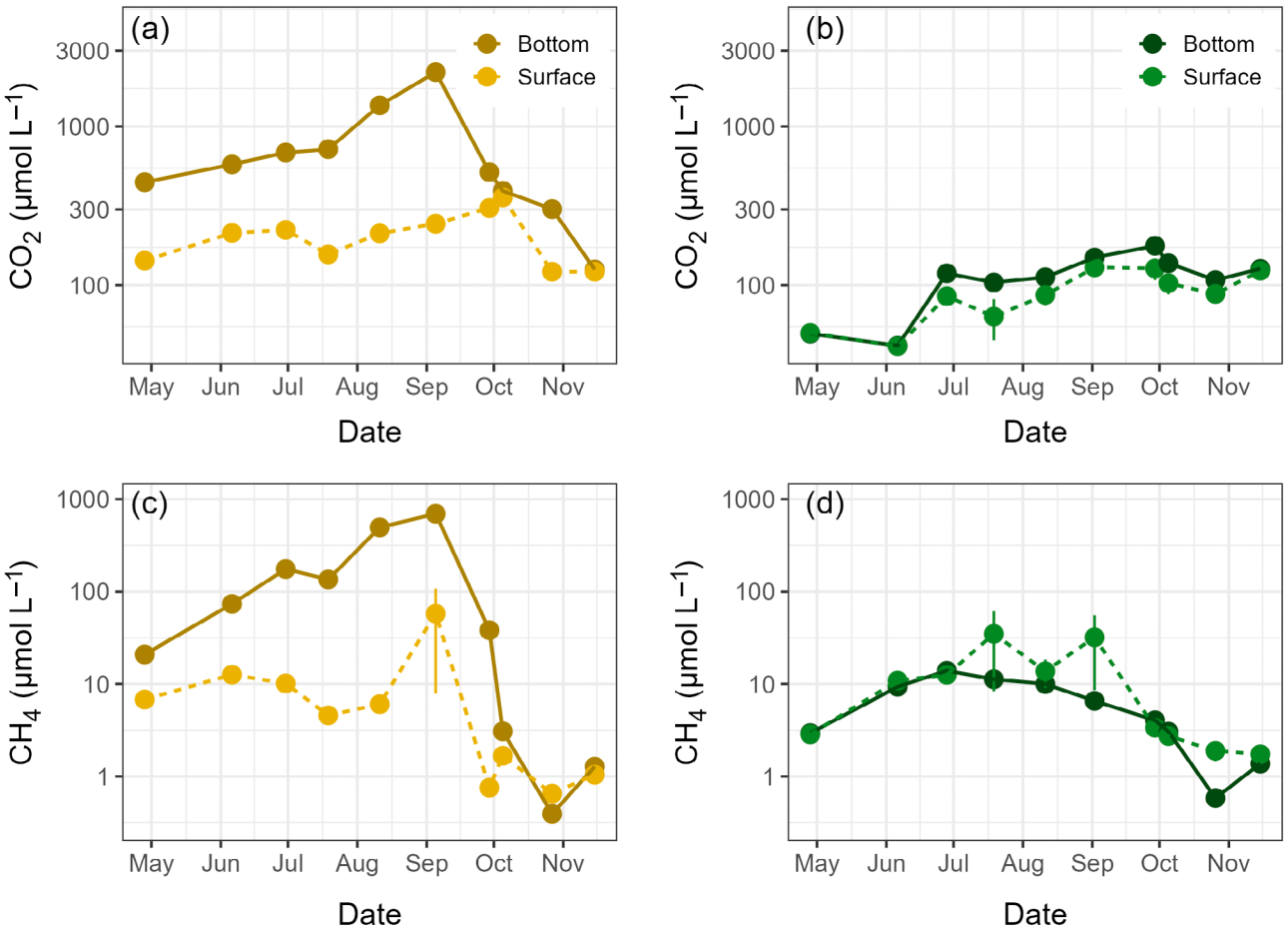

Fig. 6. Greenhouse gas (GHG) concentrations for bottom (solid lines) and surface waters (dashed lines) in Texas Hollow Pond (left; gold) and Mud Pond (right; green) for (**a**, **b**) CO_2 and (**c**, **d**) CH_4.

Greenhouse gas concentrations and fluxes

Mud Pond had similar CO_2 and CH_4 concentrations in surface and bottom waters throughout the year (Fig. 6b,d). In contrast, CO_2 and CH_4 concentrations built up in the bottom waters of Texas Hollow Pond all summer, ultimately reaching 2197.8 μmol L^{-1} for CO_2 and 695.2 μmol L^{-1} for CH_4 (Fig. 6a,c). The surface water CO_2 concentrations (Fig. 6), and hence diffusive flux rates (Fig. 7), in Texas Hollow Pond were often two to three times higher than in Mud Pond. For example, surface CO_2 concentrations averaged 81.2 ± 14.6 (SE) μmol L^{-1} in Mud Pond and 210.0 ± 14.5 μmol L^{-1} in Texas Hollow Pond from May until early September, prior to fall mixing. Despite a buildup of CH_4 in the bottom waters of Texas Hollow, surface CH_4 concentrations and diffusive fluxes were similar between the two ponds, with concentrations averaging 20.8 ± 5.2 (SE) μmol L^{-1} in Mud Pond and 18.2 ± 10.0 μmol L^{-1} in Texas Hollow Pond from May until early September (Figs. 6, 7). If all of the CH_4 stored in the bottom waters of Texas Hollow Pond was released during fall mixing, we estimate that 0.231 mol CH_4 was released at turnover (Table 2).

Measured CH_4 ebullition (from 13 June through 15 November) was higher in Mud Pond (24.8 ± 2.9 [SE] mmol m^{-2} d^{-1}) compared to Texas Hollow Pond (10.5 ± 1.4 mmol m^{-2} d^{-1}). Ebullitive emissions were much higher in Mud Pond in June and July, with similar emissions in late summer and fall (Fig. 7c). The ebullitive flux differences were driven by bubble volume, as the CH_4 bubble concentration was higher in Texas Hollow (seasonal average: 58.3%) compared to Mud Pond (seasonal average: 47.3%; Supporting Information Fig. S6).

Annual carbon fluxes

On an annual basis, Texas Hollow Pond emitted 23.14 mol C m^{-2} yr^{-1} compared to 12.78 mol C m^{-2} yr^{-1} emitted from Mud Pond (Table 2). On a molar basis, CO_2 comprised 86% of C emissions from Texas Hollow and 60% from Mud Pond. The high CO_2 emissions from Texas Hollow Pond resulted in a three times higher CO_2 : CH_4 diffusive flux ratio (15.32) compared to Mud Pond (4.96). The majority of CH_4 emissions came from ebullition in both ponds, with ebullition accounting for 70% of CH_4 emitted in Mud Pond and 53–57% of CH_4 emitted in Texas Hollow Pond, depending on if the fall turnover estimate is included. If fall turnover released all the stored benthic CH_4 from

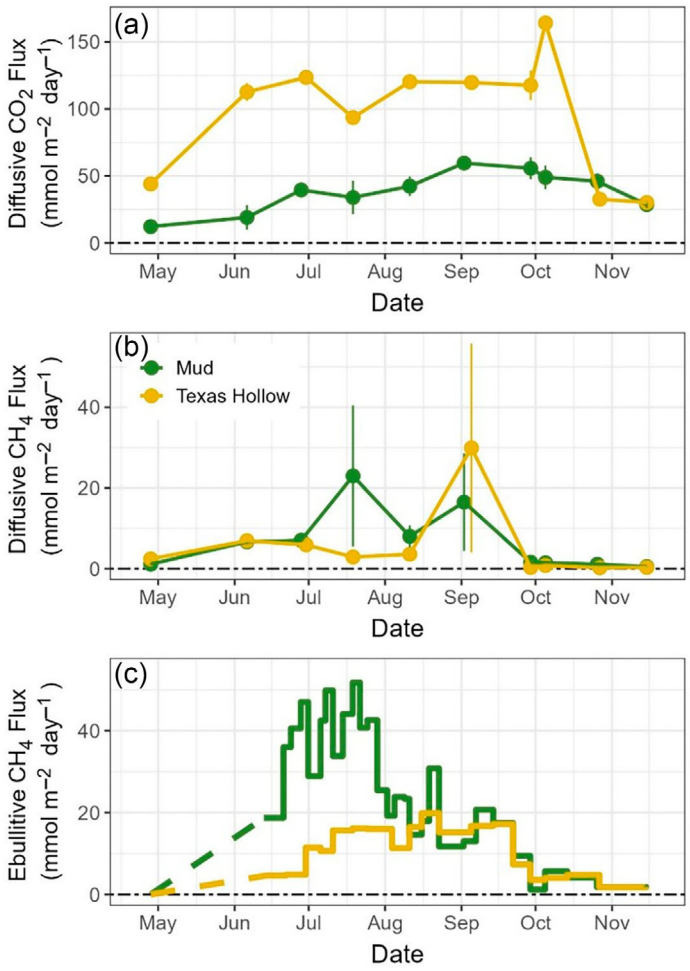

Fig. 7. Estimated greenhouse gas (GHG) flux to the atmosphere from Texas Hollow Pond (gold) and Mud Pond (green) for (**a**) diffusive CO_2, (**b**) diffusive CH_4, and (**c**) ebullitive CH_4. Error bars in (**a**) and (**b**) represent SE. Dashed lines in (**c**) represent estimated fluxes (*see* text). Black dot-dashed line indicates no net flux.

Texas Hollow Pond, it would account for 7% of the annual CH_4 emissions.

Despite emitting more C, Texas Hollow Pond also stored more C (20.44 mol C m^{-2} yr^{-1}) in the sediments compared to Mud Pond (15.23 mol C m^{-2} yr^{-1}). As such, Texas Hollow Pond was a net source to the atmosphere (2.70 mol C m^{-2} yr^{-1}), whereas Mud Pond was a net sink (− 2.45 mol C m^{-2} yr^{-1}) on a molar balance basis (not considering downstream export).

Discussion

Our two study ponds were similar in size and topography, yet a relatively small difference in z_{max} (1.2 m) and water color altered stratification, primary producer communities, and ultimately C cycling (Fig. 8). The deeper, darker waters of Texas Hollow Pond led to nearly 2 months longer and nearly two times stronger stratification than Mud Pond, resulting in anoxic bottom waters, CH_4 storage at depth, and enhanced OC burial and CO_2 emissions. In contrast, Mud Pond had weaker stratification, warmer bottom waters (+3.2°C from May to August), an oxic water column, and light that penetrated to the sediments. Consequently, Mud Pond had extensive macrophyte growth, which fueled organic matter decomposition and methanogenesis.

Table 2. Annual molar carbon (C) budget for atmospheric fluxes and sequestration for Texas Hollow Pond and Mud Pond. Standard error estimates are included for diffusive GHG fluxes and organic carbon (OC) burial. Spring ebullition rates were estimated between 28 April and 13 June (*see* Methods). The budget does not include any C from inflows or outflows (*see* Methods).

	Molar flux (mol m^{-2} yr^{-1})	
	Texas Hollow	**Mud Pond**
C flux to atmosphere		
CO_2	19.868 ± 0.380	7.639 ± 0.546
CH_4—diffusive	1.297 ± 0.311	1.541 ± 0.478
CH_4—ebullitive	1.615	3.094
CH_4—spring ebullitive, est.	0.127	0.505
CH_4—fall turnover	0.231	NA
Total C emissions	23.138	12.778
OC burial (1975–2000 average)	20.440 ± 0.958	15.228 ± 0.250
Net flux (emissions—burial)	2.698	−2.450

Carbon burial rates relate to anoxia and temperature

Carbon burial rates (182.9 and 245.5 g OC m^{-2} yr^{-1} from 1975 to 2000) in these two natural ponds were an order of magnitude greater than the average for north temperate lakes (15.0 g OC m^{-2} yr^{-1}; Heathcote et al. 2015) and higher than or similar to artificial ponds (reviewed in Holgerson et al. 2024). Texas Hollow Pond had higher OC burial, where the greater OC content offset lower accumulation rates compared to Mud Pond. While OC burial rates are understudied in ponds compared to lakes, the mechanisms are likely similarly related to oxygen availability, temperature, and organic matter quality and quantity.

We suspect that oxygen and temperature most strongly influenced OC burial in our two ponds. Specifically, the higher OC burial in Texas Hollow Pond likely reflects the cold, anoxic bottom waters compared to warmer, oxic bottom waters in Mud Pond. The deepest part of Texas Hollow was consistently hypoxic or anoxic, indicating a very short oxygen exposure time that can drastically slow decomposition and increase OC burial efficiency (Sobek et al. 2009). The colder temperatures in Texas Hollow Pond will further slow decomposition (Gudasz et al. 2010; Bartosiewicz et al. 2019).

Organic matter quality and quantity can also influence OC burial. We did not discern differences in OC quality; C : N ratios every 10 cm through the core were similar in Mud (12.7 ± 0.1 SE) and Texas Hollow (12.1 ± 0.3). However, sediment

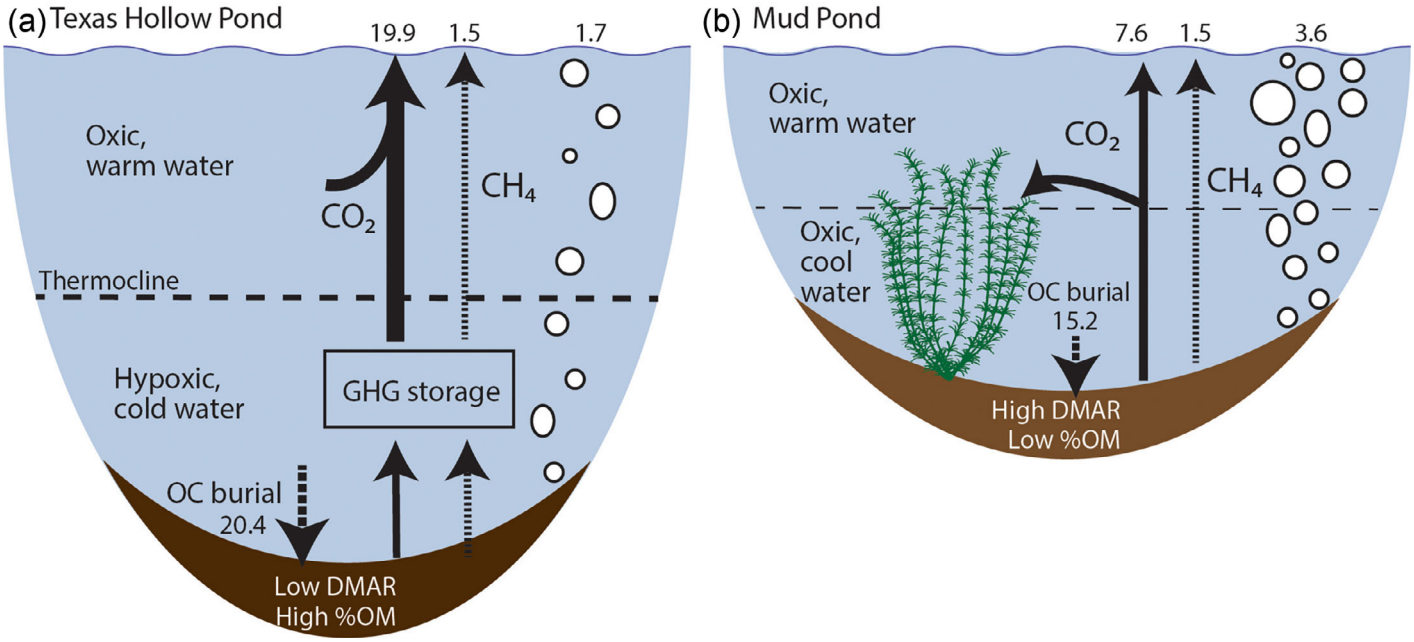

Fig. 8. Conceptual diagram of carbon fluxes in (**a**) Texas Hollow Pond that is strongly stratified and (**b**) Mud Pond that is weakly stratified with macrophytes (horizontal dashed lines indicate thermocline, with thickness indicating stratification strength). Vertical lines show net fluxes of CO_2 (solid), CH_4 (thin dashed), and OC burial (thick dashed). Sediment color reflects greater OC content in Texas Hollow Pond; DMAR stands for dry mass accumulation rate, and %OM stands for percent organic matter. Numbers, arrow width, and bubble number indicate flux estimates. Diffusive CH_4 emissions from Texas Hollow include fall turnover (Table 2). We did not measure sediment GHG production so arrow width leading to GHG storage in Texas Hollow Pond is unknown; water column CH_4 oxidation is also unknown.

loads (as measured by DMAR) were more than double in Mud compared to Texas Hollow, running counter to the trends in OC burial. The DMAR in Mud Pond increased through time (Fig. 5b), which may relate to runoff. In a description of Mud Pond from the 1920s, Needham (1921) mentioned landscape erosion, and suggested the pond could fill in by the 1970s. While the pond has yet to fill in, catchment development for agriculture, a golf course, and residential land likely contributed to increasing DMAR and OC burial, as seen in lakes globally (Heathcote et al. 2015; Anderson et al. 2020). To a lesser extent, aquatic macrophytes may facilitate increased DMAR in Mud Pond (Holgerson et al. 2024, but *see* Hilt et al. 2017). A greater pond sample size would further help link stratification, anoxia, temperature, and macrophyte biomass to OC burial mechanisms. We may even expect greater OC burial in natural ponds with high DMAR and OC content, as these factors offset each other in our two study ponds.

Carbon dioxide concentrations and fluxes relate to respiration and macrophytes

We hypothesized that Mud Pond, with its weak stratification and oxic water column, would be dominated by aerobic respiration that would cause more CO_2 emissions relative to CH_4, whereas the stratification and anoxic bottom waters of Texas Hollow Pond would lead to more CH_4 emissions relative to CO_2 (Bartosiewicz et al. 2015). Our findings indicate the opposite occurred: CO_2 concentrations and fluxes in Texas Hollow were typically double those of Mud Pond. While the CO_2 concentrations and fluxes in Mud Pond were typical for ponds of its size, the CO_2 concentrations and fluxes in Texas Hollow Pond were almost three times higher than the average for similarly sized ponds (Holgerson and Raymond 2016). The difference in CO_2 between the two ponds may be due to (1) increased lateral inputs driving greater respiration rates in Texas Hollow Pond, and (2) greater CO_2 uptake by macrophytes in Mud Pond.

First, wetlands typically load DOC into adjacent waters, resulting in a browner color and substrate for respiration in the recipient waterbody. Both study ponds were surrounded by wetlands, but Texas Hollow Pond had nearly 1 ha more wetland complex than Mud Pond and its darker color suggests relatively more wetland DOC inputs. The respiration of allochthonous DOC can drive CO_2 supersaturation (Ojala et al. 2011; Lapierre and del Giorgio 2012), which may help to explain the high ER rates along with higher CO_2 concentrations and fluxes in Texas Hollow Pond. Additionally, residence time may interact with DOC inputs. Texas Hollow Pond likely has a longer residence time than Mud Pond given its lack of a noticeable inflow and outflow. If this is correct, Texas Hollow Pond may mineralize more DOC whereas Mud Pond may export more DOC (Hanson et al. 2011), further explaining the higher CO_2 concentrations and fluxes in Texas Hollow.

Second, aquatic primary producers consume CO_2 thereby lowering CO_2 concentrations and fluxes in waterbodies (Grasset et al. 2020). While both ponds were productive, Mud Pond's oxygen supersaturation (Fig. 3) and slightly higher GPP (Fig. 4a,b) indicate high productivity by submerged macrophytes growing throughout the water column. Macrophyte beds can be highly productive, resulting in supersaturated oxygen concentrations (Andersen et al. 2017; Sand-Jensen et al. 2019) coupled with a large CO_2 demand (Ray and Holgerson 2023). Future research with larger sample sizes should explore how DOC source, macrophytes, phytoplankton, and other factors (e.g., depth, residence time) may interact to impact CO_2 production and emissions.

In addition to differences in surface water CO_2 concentrations and atmospheric fluxes, Texas Hollow Pond had bottom water CO_2 concentrations that reached an order of magnitude higher than Mud Pond (Fig. 6). Weak stratification coupled with benthic primary production limits the buildup of CO_2 in Mud Pond. In contrast, stratification coupled with high aerobic and anaerobic respiration can yield high CO_2 concentrations (Kortelainen et al. 2006), which also explains the declining pH with depth in Texas Hollow. It would be interesting for future work to examine the contributions of aerobic vs. anaerobic (e.g., denitrification, sulfate reduction) respiration in stimulating the CO_2 buildup in bottom waters.

Methane concentrations and fluxes relate to depth, temperature, and macrophytes

Both ponds were supersaturated in CH_4 for the entire study with similar surface concentrations and diffusive emissions, but ebullitive CH_4 flux was twice as high in Mud Pond compared to Texas Hollow Pond (Table 2). Summertime concentrations (averages: 18.2–20.7 μmol L^{-1}) and diffusive fluxes (averages: 9.85–12.2 mmol m^{-2} d^{-1}) were on the high end of the range observed in similarly sized ponds globally (Rosentreter et al. 2021; Rabaey and Cotner 2022). Ebullitive CH_4 fluxes were higher than mean values reported from other ponds, with Texas Hollow Pond falling on the upper range and Mud Pond having among the highest reported ebullitive fluxes (reviewed in Rabaey and Cotner 2022 and Baron et al. 2022). Our observed CH_4 dynamics reflect production, transport, and oxidation pathways that likely differed between the two ponds.

The extremely high ebullitive flux in Mud Pond suggests higher CH_4 production than Texas Hollow Pond. Methane production tends to increase with higher quality and quantity of organic matter inputs, anoxic conditions, and warmer temperatures (Yvon-Durocher et al. 2014; Grasset et al. 2018). While we expected that the greater sediment OC content and anoxic bottom waters in Texas Hollow would promote methanogenesis, it appears that the warmer temperatures and macrophyte loads in Mud Pond may play a larger role. Water column oxygen may not be as important given that oxygen may not penetrate more than a few mm to 1 cm into the sediments (Sobek et al. 2017). Rather, Mud Pond's bottom temperatures were typically > 15°C (Fig. 2b), averaging 3.2°C warmer than Texas Hollow in the summer, which could result in ~ 25% difference in CH_4 production given the bottom water temperatures we observed (Aben et al. 2017).

We suspect that differences in organic matter loads also contributed to differences in CH_4 production and observed ebullition between the ponds. While senesced macrophytes and phytoplankton can yield similar CO_2 and CH_4 production (Grasset et al. 2018, 2021), they may differ in the quantity of organic matter reaching the sediments. At high densities, macrophytes can self-shade, slough tissue, and fuel respiration near the sediments even as growth occurs higher in the water column (Theus et al. 2023). In contrast, phytoplankton may partially decompose in the water column before reaching the sediments, leading macrophytes to potentially fuel greater ebullition (Wik et al. 2013; Bauduin et al. 2025). It seems likely that the macrophytes in Mud Pond delivered more organic matter to sediments than phytoplankton in Texas Hollow, thereby fueling CH_4 ebullition. Lastly, depth affects hydrostatic pressure, often causing greater ebullition when depths are < 2 m (DelSontro et al. 2016). However, the 1.2 m difference in z_{max} we observed equates to minor (0.1 atm) changes in hydrostatic pressure, which should have minimal effects on ebullition rates (Sø et al. 2023).

Unlike ebullition, we observed similar surface CH_4 concentrations and diffusive fluxes between our two study ponds, supporting studies that found increased CH_4 production or ebullition does not necessarily increase diffusive emissions (West et al. 2016; Bauduin et al. 2025). Surface CH_4 concentrations and fluxes may not align with production due to CH_4 storage, transport, or oxidation processes, which we did not assess. We suspect that CH_4 storage in the bottom waters of Texas Hollow reflects strong stratification that limits CH_4 evasion to the atmosphere. While other studies found stratification increased CH_4 concentrations in both bottom and surface waters of shallow waterbodies (Ray and Holgerson 2023; Davidson et al. 2024), those waterbodies were either larger (11 ha; Davidson et al. 2024) or shallower (2.1 m; Ray and Holgerson 2023) than Texas Hollow Pond with intermittent summertime mixing, suggesting greater gas exchange across the water column. Methane oxidation may also differ among the ponds. The oxygenated waters of Mud Pond may favor CH_4 oxidation, and macrophytes can host methanotrophs (Yoshida et al. 2014). Yet, the shallower water column and potentially shorter residence time in Mud Pond may reduce opportunities for oxidation as CH_4 moves through the water column. Ultimately, our comparative study of two ponds suggests that temperature and macrophytes play an important role in CH_4 production and ebullition, but that further study is needed across a larger number of ponds to understand how stratification influences CH_4 storage and transport.

Annual carbon budget and uncertainties

For both ponds, the annual flux of C gases to the atmosphere (23.1 and 12.8 mol m^{-2} yr^{-1} in Texas Hollow and Mud Ponds, respectively) is similar to sediment OC burial (20.4 and 15.2 mol m^{-2} yr^{-1}) on a molar basis (Table 2). This contrasts with many other lentic systems where atmospheric C emissions are often more than double the rate of OC burial (Cole et al. 2007; Tranvik et al. 2009) and indicates that some ponds may trap and bury more C than they emit or export. It is important to note that we do not have constrained estimates of C inputs or outputs for either pond, despite the fact that both have low or intermittent hydrologic connectivity.

Our annual flux estimates come with uncertainties that should be explored further. First, we assumed that all CH_4 stored in the bottom waters of Texas Hollow Pond was emitted at fall turnover despite the fact that some oxidation likely took place. Yet as the CH_4 emissions from fall turnover were low (< 1% of all C emitted and 7% of all CH_4 emitted on a molar basis), our study indicates that deeper waters with strong stratification may reduce CH_4 emissions. Second, we did not assess emissions at ice melt. We expect fluxes at ice melt to make a small contribution to annual emissions due to lower production with cold temperatures, especially relative to the high summertime emissions we observed. Lastly, the timescale of our measurements poses challenges. We assumed GHG fluxes were similar over a diel cycle, but CO_2 fluxes may be greater at night from respiration while CH_4 emissions can vary on diel cycles due to convective cooling, wind, and temperature (Sieczko et al. 2020; Sø et al. 2024). Additionally, C burial is estimated on the scale of years to decades and GHGs were measured on individual days within 1 yr. While we work to better resolve these uncertainties, we contend that our study helps to identify mechanisms of C processing, including what factors make ponds net sources or sinks for OC. Considering that small lakes and ponds may be particularly sensitive to climate-driven changes in stratification (Winslow et al. 2015; Bartosiewicz et al. 2019), there is a strong need to mechanistically untangle the drivers of C flux in these systems.

Author Contributions

Meredith A. Holgerson conceived the study, secured funding, and led data analysis and manuscript writing. Nicholas E. Ray and Kathryn A. Gannon led field work with support from Meredith A. Holgerson. Adam J. Heathcote led sediment coring, with support from Meredith A. Holgerson and Nicholas E. Ray. All authors contributed to data processing, data analysis, and writing/editing the manuscript.

Acknowledgments

We are grateful to Daniel Consolvo, Lee Fitzgerald, Wulfgar Ramsey, Peri Cooper, Beatriz Moreira Ferreira, Chelsea Russ, and Meredith Theus for field or lab work assistance. Thank you to Benj Sterrett for constructing our coring outrigger, Brian Brown for help constructing bubble traps, Ellie Socha for water color data and collecting macrophyte specimens, and Kim Sparks and the Cornell University Stable Isotope Facility (COIL) for analyzing sediment C : N content. We thank Cornell Botanical Gardens Natural Areas for access to Mud Pond and the New York State Department of Environmental Conservation Region 8 for permission to sample within Texas Hollow State Forest. This manuscript benefitted from three anonymous reviews. This study was funded by the New York State Water Resources Institute and the National Science Foundation (Grant 2143449).

Conflicts of Interest

None declared.

Data Availability Statement

The data associated with this paper can be found at Dryad: https://doi.org/10.5061/dryad.ksn02v7dp.

References

Aben, R. C. H., N. Barros, E. van Donk, et al. 2017. "Cross Continental Increase in Methane Ebullition Under Climate Change." *Nature Communications* 8: 1682. https://doi.org/10.1038/s41467-017-01535-y.

Andersen, M. R., T. Kragh, and K. Sand-Jensen. 2017. "Extreme Diel Dissolved Oxygen and Carbon Cycles in Shallow Vegetated Lakes." *Proceedings of the Royal Society B: Biological Sciences* 284: 20171427. https://doi.org/10.1098/rspb.2017.1427.

Anderson, N. J., A. J. Heathcote, D. R. Engstrom, and Globocarb Data Contributors. 2020. "Anthropogenic Alteration of Nutrient Supply Increases the Global Freshwater Carbon Sink." *Science Advances* 6: eaaw2145. https://doi.org/10.1126/sciadv.aaw2145.

Appleby, P. G. 2001. "Chronostratigraphic Techniques in Recent Sediments." In Tracking Environmental Change Using Lake Sediments: Basin Analysis, Coring, and Chronological Techniques, edited by W. M. Last and J. P. Smol, 171–203. Netherlands: Springer.

Baliña, S., M. L. Sánchez, I. Izaguirre, and P. A. del Giorgio. 2023. "Shallow Lakes Under Alternative States Differ in the Dominant Greenhouse Gas Emission Pathways." *Limnology and Oceanography* 68: 1–13. https://doi.org/10.1002/lno.12243.

Baron, A. A. P., L. T. Dyck, H. Amjad, et al. 2022. "Differences in Ebullitive Methane Release from Small, Shallow Ponds Present Challenges for Scaling." *Science of The Total Environment* 802: 149685. https://doi.org/10.1016/j.scitotenv.2021.149685.

Bartosiewicz, M., A. Przytulska, J. Lapierre, I. Laurion, M. F. Lehmann, and R. Maranger. 2019. "Hot Tops, Cold

Bottoms: Synergistic Climate Warming and Shielding Effects Increase Carbon Burial in Lakes." *Limnology and Oceanography* 4: 132–144. https://doi.org/10.1002/lol2.10117.

Bartosiewicz, M., I. Laurion, and S. MacIntyre. 2015. "Greenhouse Gas Emission and Storage in a Small Shallow Lake." *Hydrobiologia* 757: 101–115. https://doi.org/10.1007/s10750-015-2240-2.

Bauduin, T., N. Gypens, and A. V. Borges. 2025. "Methane, Carbon Dioxide, and Nitrous Oxide Emissions From Two Clear-Water and Two Turbid-Water Urban Ponds in Brussels (Belgium)." *Biogeosciences* 22: 3785–3805. https://doi.org/10.5194/bg-22-3785-2025.

Cole, J. J., D. L. Bade, D. Bastviken, M. L. Pace, and M. Van de Bogert. 2010. "Multiple Approaches to Estimating Air–Water Gas Exchange in Small Lakes." *Limnology and Oceanography: Methods* 8: 285–293. https://doi.org/10.4319/lom.2010.8.285.

Cole, J. J., and N. F. Caraco. 1998. "Atmospheric Exchange of Carbon Dioxide in a Low-Wind Oligotrophic Lake Measured by the Addition of SF6." *Limnology and Oceanography* 43: 647–656. https://doi.org/10.4319/lo.1998.43.4.0647.

Cole, J. J., Y. T. Prairie, N. F. Caraco, et al. 2007. "Plumbing the Global Carbon Cycle: Integrating Inland Waters into the Terrestrial Carbon Budget." *Ecosystems* 10: 172–185. https://doi.org/10.1007/s10021-006-9013-8.

Davidson, T. A., M. Søndergaard, J. Audet, et al. 2024. "Temporary Stratification Promotes Large Greenhouse Gas Emissions in a Shallow Eutrophic Lake." *Biogeosciences* 21: 93–107. https://doi.org/10.5194/bg-21-93-2024.

Dean, W. E. 1974. "Determination of Carbonate and Organic Matter in Calcareous Sediments and Sedimentary Rocks by Loss on Ignition; Comparison With Other Methods." *Journal of Sedimentary Research* 44: 242–248. https://doi.org/10.1306/74D729D2-2B21-11D7-8648000102C1865D.

Deemer, B. R., and M. A. Holgerson. 2021. "Drivers of Methane Flux Differ Between Lakes and Reservoirs, Complicating Global Upscaling Efforts." *JGR Biogeosciences* 126: e2019JG005600. https://doi.org/10.1029/2019JG005600.

DelSontro, T., L. Boutet, A. St-Pierre, P. A. del Giorgio, and Y. T. Prairie. 2016. "Methane Ebullition and Diffusion From Northern Ponds and Lakes Regulated by the Interaction Between Temperature and System Productivity." *Limnology and Oceanography* 61: S62–S77. https://doi.org/10.1002/lno.10335.

Downing, J. 2010. "Emerging Global Role of Small Lakes and Ponds: Little Things Mean a Lot." *Limnetica* 29: 9–24. https://doi.org/10.23818/limn.29.02.

Downing, J. A., J. J. Cole, J. J. Middelburg, et al. 2008. "Sediment Organic Carbon Burial in Agriculturally Eutrophic Impoundments Over the Last Century: Sediment Organic Carbon Burial." *Global Biogeochemical Cycles* 22: GB1018. https://doi.org/10.1029/2006GB002854.

Eakins, J. D., and R. T. Morrison. 1978. "A New Procedure for the Determination of Lead-210 in Lake and Marine Sediments." *International Journal of Applied Radiation and Isotopes* 29: 531–536. https://doi.org/10.1016/0020-708X(78)90161-8.

Fee, E. J., R. E. Hecky, S. E. M. Kasian, and D. R. Cruikshank. 1996. "Effects of Lake Size, Water Clarity, and Climatic Variability on Mixing Depths in Canadian Shield Lakes." *Limnology and Oceanography* 41: 912–920. https://doi.org/10.4319/lo.1996.41.5.0912.

Gebhardt, A., R. Bivand, and D. Sinclair. 2024. interp: Interpolation Methods. R package version 1.1-6. https://cran.r-project.org/package=interp.

Grasset, C., R. Mendonça, G. Villamor Saucedo, D. Bastviken, F. Roland, and S. Sobek. 2018. "Large But Variable Methane Production in Anoxic Freshwater Sediment Upon Addition of Allochthonous and Autochthonous Organic Matter: Methanogenic Potential of Different OC Types." *Limnology and Oceanography* 63: 1488–1501. https://doi.org/10.1002/lno.10786.

Grasset, C., S. Moras, A. Isidorova, R. Couture, A. Linkhorst, and S. Sobek. 2021. "An Empirical Model to Predict Methane Production in Inland Water Sediment From Particular Organic Matter Supply and Reactivity." *Limnology and Oceanography* 66: 3643–3655. https://doi.org/10.1002/lno.11905.

Grasset, C., S. Sobek, K. Scharnweber, et al. 2020. "The CO_2-Equivalent Balance of Freshwater Ecosystems Is Non-Linearly Related to Productivity." *Global Change Biology* 26: 5705–5715. https://doi.org/10.1111/gcb.15284.

Gray, E., E. B. Mackay, J. A. Elliott, A. M. Folkard, and I. D. Jones. 2020. "Wide-Spread Inconsistency in Estimation of Lake Mixed Depth Impacts Interpretation of Limnological Processes." *Water Research* 168: 115136. https://doi.org/10.1016/j.watres.2019.115136.

Gudasz, C., D. Bastviken, K. Steger, K. Premke, S. Sobek, and L. J. Tranvik. 2010. "Temperature-Controlled Organic Carbon Mineralization in Lake Sediments." *Nature* 466: 478–481. https://doi.org/10.1038/nature09186.

Hanson, P. C., D. P. Hamilton, E. H. Stanley, N. Preston, O. C. Langman, and E. L. Kara. 2011. "Fate of Allochthonous Dissolved Organic Carbon in Lakes: A Quantitative Approach." *PLoS One* 6: e21884. https://doi.org/10.1371/journal.pone.0021884.

Heathcote, A. J., N. J. Anderson, Y. T. Prairie, D. R. Engstrom, and P. A. del Giorgio. 2015. "Large Increases in Carbon Burial in Northern Lakes During the Anthropocene." *Nature Communications* 6: 10016. https://doi.org/10.1038/ncomms10016.

Heathcote, A. J., and J. A. Downing. 2012. "Impacts of Eutrophication on Carbon Burial in Freshwater Lakes in an Intensively Agricultural Landscape." *Ecosystems* 15: 60–70. https://doi.org/10.1007/s10021-011-9488-9.

Hilt, S., S. Brothers, E. Jeppesen, A. J. Veraart, and S. Kosten. 2017. "Translating Regime Shifts in Shallow Lakes into Changes in Ecosystem Functions and Services." *Bioscience* 67: 928–936. https://doi.org/10.1093/biosci/bix106.

Holgerson, M. A., E. R. Farr, and P. A. Raymond. 2017. "Gas Transfer Velocities in Small Forested Ponds." *Journal of Geophysical Research* 122: 1011–1021. https://doi.org/10.1002/2016JG003734.

Holgerson, M. A., N. E. Ray, and C. Russ. 2024. "High Rates of Carbon Burial Linked to Autochthonous Production in Artificial Ponds." *Limnology and Oceanography Letters* 9: 43–51. https://doi.org/10.1002/lol2.10351.

Holgerson, M. A., and P. A. Raymond. 2016. "Large Contribution to Inland Water CO_2 and CH_4 Emissions From Very Small Ponds." *Nature Geoscience* 9: 222–226. https://doi.org/10.1038/ngeo2654.

Holgerson, M. A., D. C. Richardson, J. Roith, et al. 2022. "Classifying Mixing Regimes in Ponds and Shallow Lakes." *Water Resources Research* 58: e2022WR032522. https://doi.org/10.1029/2022WR032522.

Jähne, B., K. O. Münnich, R. Bösinger, A. Dutzi, W. Huber, and P. Libner. 1987. "On the Parameters Influencing Air–Water Gas Exchange." *Journal of Geophysical Research: Oceans* 92: 1937–1949. https://doi.org/10.1029/JC092iC02p01937.

Kortelainen, P., M. I. I. T. T. A. Rantakari, J. A. R. I. T. Huttunen, et al. 2006. "Sediment Respiration and Lake Trophic State Are Important Predictors of Large CO_2 Evasion From Small Boreal Lakes." *Global Change Biology* 12: 1554–1567. https://doi.org/10.1111/j.1365-2486.2006.01167.x.

Kuhn, M., M. Schmidt, L. Heffernan, et al. 2023. "High Ebullitive, Millennial-Aged Greenhouse Gas Emissions From Thermokarst Expansion of Peatland Lakes in Boreal Western Canada." *Limnology and Oceanography* 68: 498–513. https://doi.org/10.1002/lno.12288.

LaBrie, R., and R. Maranger. 2024. "Predicting the Presence of Hypoxic Hypolimnia in Lakes at Large Spatial Scales." *Limnology and Oceanography* 69: 355–366. https://doi.org/10.1002/lno.12488.

Lapierre, J.-F., and P. A. del Giorgio. 2012. "Geographical and Environmental Drivers of Regional Differences in the Lake pCO_2 Versus DOC Relationship Across Northern Landscapes." *Journal of Geophysical Research: Biogeosciences* 117: G03015. https://doi.org/10.1029/2012JG001945.

Matthews, C. J. D., V. L. St.Louis, and R. H. Hesslein. 2003. "Comparison of Three Techniques Used to Measure Diffusive Gas Exchange From Sheltered Aquatic Surfaces." *Environmental Science & Technology* 37: 772–780. https://doi.org/10.1021/es0205838.

Muir, D. C. G., X. Wang, F. Yang, et al. 2009. "Spatial Trends and Historical Deposition of Mercury in Eastern and Northern Canada Inferred From Lake Sediment Cores." *Environmental Science & Technology* 43: 4802–4809. https://doi.org/10.1021/es8035412.

Needham, J. G. 1921. "The New Wild Life Preserve near McLean, N. Y." *Scientific Monthly* 12: 246–252. https://www.jstor.org/stable/6835?seq=1.

Nürnberg, G. K. 1987. "A Comparison of Internal Phosphorus Loads in Lakes With Anoxic Hypolimnia: Laboratory Incubation Versus In Situ Hypolimnetic Phosphorus Accumulation." *Limnology and Oceanography* 32: 1160–1164. https://doi.org/10.4319/lo.1987.32.5.1160.

Ojala, A., J. L. Bellido, T. Tulonen, P. Kankaala, and J. Huotari. 2011. "Carbon Gas Fluxes From a Brown-Water and a Clear-Water Lake in the Boreal Zone During a Summer With Extreme Rain Events." *Limnology and Oceanography* 56: 61–76. https://doi.org/10.4319/lo.2011.56.1.0061.

R Core Team. 2020. The R Project for Statistical Computing. R Foundation for Statistical Computing. https://www.R-project.org/.

Rabaey, J. S., and J. B. Cotner. 2022. "Pond Greenhouse Gas Emissions Controlled by Duckweed Coverage." *Frontiers in Environmental Science* 10: 889289. https://doi.org/10.3389/fenvs.2022.889289.

Rabaey, J. S., and J. B. Cotner. 2024. "The Influence of Mixing on Seasonal Carbon Dioxide and Methane Fluxes in Ponds." *Biogeochemistry* 167: 1297–1314. https://doi.org/10.1007/s10533-024-01167-7.

Rabaey, J. S., M. A. Holgerson, D. C. Richardson, et al. 2024. "Freshwater Biogeochemical Hotspots: High Primary Production and Ecosystem Respiration in Shallow Waterbodies." *Geophysical Research Letters* 51: e2023GL106689. https://doi.org/10.1029/2023GL106689.

Ray, N. E., and M. A. Holgerson. 2023. "High Intra-Seasonal Variability in Greenhouse Gas Emissions From Temperate Constructed Ponds." *Geophysical Research Letters* 50: e2023GL104235. https://doi.org/10.1029/2023GL104235.

Ray, N. E., M. A. Holgerson, M. R. Andersen, et al. 2023. "Spatial and Temporal Variability in Summertime Dissolved Carbon Dioxide and Methane in Temperate Ponds and Shallow Lakes." *Limnology and Oceanography* 68: 1530–1545. https://doi.org/10.1002/lno.12362.

Richardson, D. C., M. A. Holgerson, M. J. Farragher, et al. 2022. "A Functional Definition to Distinguish Ponds from Lakes and Wetlands." *Scientific Reports* 12: 10472. https://doi.org/10.1038/s41598-022-14569-0.

Rosentreter, J. A., A. V. Borges, B. R. Deemer, et al. 2021. "Half of Global Methane Emissions Come From Highly Variable Aquatic Ecosystem Sources." *Nature Geoscience* 14: 225–230. https://doi.org/10.1038/s41561-021-00715-2.

Sand-Jensen, K., M. R. Andersen, K. T. Martinsen, J. Borum, E. Kristensen, and T. Kragh. 2019. "Shallow Plant-Dominated Lakes—Extreme Environmental Variability, Carbon Cycling and Ecological Species Challenges." *Annals of Botany* 124: 355–366. https://doi.org/10.1093/aob/mcz084.

Scheffer, M., S. H. Hosper, M.-L. Meijer, B. Moss, and E. Jeppesen. 1993. "Alternative Equilibria in Shallow Lakes." *Trends in Ecology & Evolution* 8: 275–279. https://doi.org/10.1016/0169-5347(93)90254-M.

Sieczko, A. K., N. T. Duc, J. Schenk, et al. 2020. "Diel Variability of Methane Emissions From Lakes." *Proceedings of the National Academy of Sciences of the United States of*

America 117: 21488–21494. https://doi.org/10.1073/pnas.2006024117.

Signorell, A. 2024. DescTools: Tools for Descriptive Statistics. R package version 0.99.60.24. https://github.com/andrisignorell/desctools.

Sø, J. S., K. Sand-Jensen, K. T. Martinsen, et al. 2023. "Methane and Carbon Dioxide Fluxes at High Spatiotemporal Resolution From a Small Temperate Lake." *Science of the Total Environment* 878: 162895. https://doi.org/10.1016/j.scitotenv.2023.162895.

Sø, J. S., K. T. Martinsen, T. Kragh, and K. Sand-Jensen. 2024. "Hourly Methane and Carbon Dioxide Fluxes From Temperate Ponds." *Biogeochemistry* 167: 177–195. https://doi.org/10.1007/s10533-024-01124-4.

Sobek, S., C. Gudasz, B. Koehler, L. J. Tranvik, D. Bastviken, and M. Morales-Pineda. 2017. "Temperature Dependence of Apparent Respiratory Quotients and Oxygen Penetration Depth in Contrasting Lake Sediments." *Journal of Geophysical Research: Biogeosciences* 122: 3076–3087. https://doi.org/10.1002/2017JG003833.

Sobek, S., E. Durisch-Kaiser, R. Zurbrügg, et al. 2009. "Organic Carbon Burial Efficiency in Lake Sediments Controlled by Oxygen Exposure Time and Sediment Source." *Limnology and Oceanography* 54: 2243–2254. https://doi.org/10.4319/lo.2009.54.6.2243.

Søndergaard, M., A. Nielsen, L. S. Johansson, and T. A. Davidson. 2023. "Temporarily Summer-Stratified Lakes Are Common: Profile Data From 436 Lakes in Lowland Denmark." *Inland Waters* 13: 153–166. https://doi.org/10.1080/20442041.2023.2203060.

Søndergaard, M., G. Phillips, S. Hellsten, et al. 2013. "Maximum Growing Depth of Submerged Macrophytes in European Lakes." *Hydrobiologia* 704: 165–177. https://doi.org/10.1007/s10750-012-1389-1.

Theus, M. E., N. E. Ray, S. Bansal, and M. A. Holgerson. 2023. "Submersed Macrophyte Density Regulates Aquatic Greenhouse Gas Emissions." *JGR Biogeosciences* 128: e2023JG007758. https://doi.org/10.1029/2023JG007758.

Tranvik, L. J., J. A. Downing, J. B. Cotner, et al. 2009. "Lakes and Reservoirs as Regulators of Carbon Cycling and Climate." *Limnology and Oceanography* 54: 2298–2314. https://doi.org/10.4319/lo.2009.54.6_part_2.2298.

Vachon, D., and Y. T. Prairie. 2013. "The Ecosystem Size and Shape Dependence of Gas Transfer Velocity Versus Wind Speed Relationships in Lakes R. Smith [Ed.]." *Canadian Journal of Fisheries and Aquatic Sciences* 70: 1757–1764. https://doi.org/10.1139/cjfas-2013-0241.

Wanninkhof, R. 1992. "Relationship Between Wind Speed and Gas Exchange Over the Ocean." *Journal of Geophysical Research: Oceans* 97: 7373–7382. https://doi.org/10.1029/92JC00188.

Weiss, R. F. 1974. "Carbon Dioxide in Water and Seawater: The Solubility of a Non-Ideal Gas." *Marine Chemistry* 2: 203–215. https://doi.org/10.1016/0304-4203(74)90015-2.

West, W. E., K. P. Creamer, and S. E. Jones. 2016. "Productivity and Depth Regulate Lake Contributions to Atmospheric Methane." *Limnology and Oceanography* 61: S51–S61. https://doi.org/10.1002/lno.10247.

Wetzel, R., and G. Likens. 2000. Limnological Analyses. 3rd ed. Springer.

Wiesenburg, D. A., and N. L. Guinasso Jr. 1979. "Equilibrium Solubilities of Methane, Carbon Monoxide, and Hydrogen in Water and Sea Water." *Journal of Chemical and Engineering Data* 24: 356–360. https://doi.org/10.1021/je60083a006.

Wik, M., P. M. Crill, R. K. Varner, and D. Bastviken. 2013. "Multiyear Measurements of Ebullitive Methane Flux From Three Subarctic Lakes." *Journal of Geophysical Research: Biogeosciences* 118: 1307–1321. https://doi.org/10.1002/jgrg.20103.

Winslow, L. A., J. S. Read, G. J. A. Hansen, and P. C. Hanson. 2015. "Small Lakes Show Muted Climate Change Signal in Deepwater Temperatures." *Geophysical Research Letters* 42: 355–361. https://doi.org/10.1002/2014GL062325.

Winslow, L. A., J. A. Zwart, R. D. Batt, et al. 2016. "LakeMetabolizer: An R Package for Estimating Lake Metabolism From Free-Water Oxygen Using Diverse Statistical Models." *Inland Waters* 6: 622–636. https://doi.org/10.1080/IW-6.4.883.

Wright, H. E. 1991. "Coring Tips." *Journal of Paleolimnology* 6: 37–49. https://doi.org/10.1007/BF00201298.

Yentsch, C. S., and D. W. Menzel. 1963. "A Method for the Determination of Phytoplankton Chlorophyll and Phaeophytin by Fluorescence." *Deep Sea Research and Oceanographic Abstracts* 10: 221–231. https://doi.org/10.1016/0011-7471(63)90358-9.

Yoshida, N., H. Iguchi, H. Yurimoto, A. Murakami, and Y. Sakai. 2014. "Aquatic Plant Surface as a Niche for Methanotrophs." *Frontiers in Microbiology* 5: 30. https://doi.org/10.3389/fmicb.2014.00030.

Yvon-Durocher, G., A. P. Allen, D. Bastviken, et al. 2014. "Methane Fluxes Show Consistent Temperature Dependence Across Microbial to Ecosystem Scales." *Nature* 507: 488–491. https://doi.org/10.1038/nature13164.

Supporting Information

Additional Supporting Information may be found in the online version of this article.

Submitted 09 June 2025
Revised 21 October 2025
Accepted 07 November 2025